CORE
Metadata, citation and similar papers at core.ac.uk
Provided by DSpace@MIT

Laser direct write system for fabricating seamless roll-to-roll lithography tools

Joseph E. Petrzelka and David E. Hardt

Massachusetts Institute of Technology
77 Massachusetts Ave, Cambridge, Massachusetts, United States

ABSTRACT

Implementations of roll to roll contact lithography require new approaches towards manufacturing tooling, including stamps for roll to roll nanoimprint lithography (NIL) and soft lithography. Suitable roll based tools must have seamless micro- or nano-scale patterns and must be scalable to roll widths of one meter. The authors have developed a new centrifugal stamp casting process that can produce uniform cylindrical polymer stamps in a scalable manner. The pattern on the resulting polymer tool is replicated against a corresponding master pattern on the inner diameter of a centrifuge drum. This master pattern is created in photoresist using a UV laser direct write system. This paper discusses the design and implementation of a laser direct write system targeting the internal diameter of a rotating drum. The design uses flying optics to focus a laser beam along the axis of the centrifuge drum and to redirect the beam towards the drum surface. Experimental patterning results show uniform coatings of negative photoresist in the centrifuge drum that are effectively patterned with a 405 nm laser diode. Seamless patterns are shown to be replicated in a 50 mm diameter, 60 mm long cylindrical stamp made from polydimethylsiloxane (PDMS). Direct write results show gratings with line widths of 10 microns in negative photoresist. Using an FPGA, the laser can be accurately timed against the centrifuge encoder to create complex patterns.

Keywords: Nanoimprint lithography, Soft lithography, Direct write, Centrifugal casting, Flexible electronics, Patterning, Laser

1. INTRODUCTION

Roll to roll lithography has the potential to enable low cost, high rate manufacturing of flexible electronics and engineered metasurfaces. High resolution patterned tooling remains a major challenge in developing these roll based techniques, including nanoimprint lithography (NIL)[1] and soft lithography.[2] Roll based tooling has been approached from two perspectives: (*i*) well developed planar processing techniques are used to prepare a shim that is wrapped around a roll or (*ii*) seamless cylindrical tools are created using modified lithographic techniques.[3] Seamless cylindrical tools have the advantage of printing repeated patterns over indefinite lengths of substrate. If these tools can be produced with the same resolution and accuracy as planar processing techniques, they would be the preferred choice for roll based printing.

Methods of producing seamless roll tooling in the literature have used lithographic means to pattern the outer diameter of a metal roll for NIL. Different approaches have used ultraviolet (UV),[4,5] x-ray,[6] or electron beam[7–9] sources to pattern a photoresist layer. The patterned photoresist can then be used directly for imprinting or act as a mask for etching or deposition of more durable metal patterns.

These reported techniques can be slow and scale poorly (especially if using electron beam) and the lithographic process must be repeated on each tool. Photoresist is most commonly applied by dip coating the roll, which may result in variable coating thickness. While a rigid metal tool is preferable for certain nanoimprint processes, these approaches cannot produce a polymer tool, for example elastomeric tools that are preferable for soft lithography or high resolution flexography.

Viable methods for producing seamless polymer stamps must provide (*i*) economical production rates, (*ii*) scalable nature, and (*iii*) macroscopic dimensional precision. Fast production rates are required for polymer stamps, which have a limited lifetime and must be replaced more frequently than metal imprint tools. The production method must rely on processes that can be scaled to rolls that may be a meter or more in length. Recent studies have shown the need for tight stamp thickness tolerances to maintain stamp contact fidelity.[10,11]

Micromachining and Microfabrication Process Technology XVIII, edited by Mary Ann Maher, Paul J. Resnick,
Proc. of SPIE Vol. 8612, 861205 · © 2013 SPIE · CCC code: 0277-786X/13/$18 · doi: 10.1117/12.2004738

Downloaded From: http://proceedings.spiedigitallibrary.org/ on 06/17/2015 Terms of Use: http://spiedl.org/terms

Towards these goals, the authors have developed a new method of producing cylindrical polymer stamps, with a focus on polydimethylsiloxane (PDMS) stamps appropriate for microcontact printing, nanoimprint lithography, or high resolution flexography. This method uses a patterned centrifuge drum as a cylindrical master template, allowing centrifugal casting of a patterned polymer stamp (Figure 1). The cured polymer stamp can be removed from the centrifuge drum and applied to a roll using a thin film of pressurized air or solvent. This method is capable of producing a cylindrical polymer stamp with continuously patterned features on the outer diameter and an exceptionally uniform thickness.

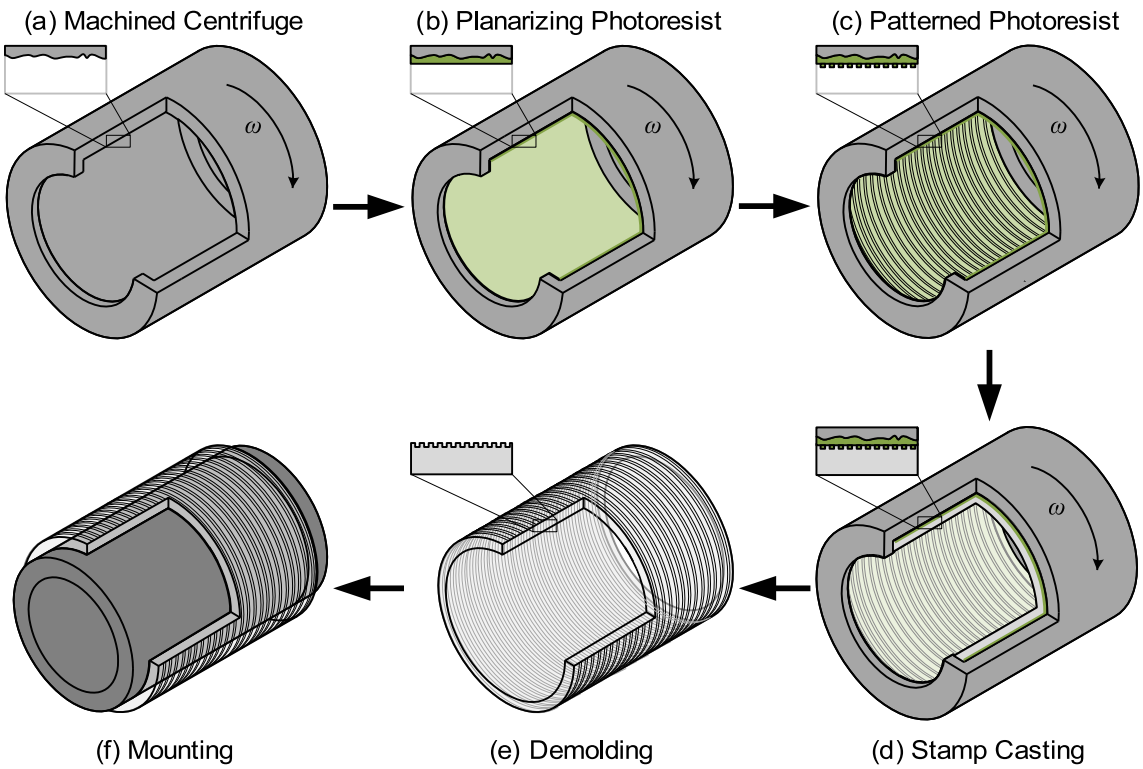

Figure 1: Process map showing production of cylindrical polymer stamps. (a) A machined centrifuge drum is (b) coated with a uniform layer of photoresist to planarize the surface. (c) A second layer of photoresist is patterned inside the drum to create a relief pattern. (d) A polymer precursor is cast inside the centrifuge drum, creating a cylindrical stamp with surface relief features. Finally, (e) the stamp is demolded from the centrifuge drum and (f) mounted to a shaft for use as a roll-to-roll printing tool.

This paper focuses on the production of the patterned centrifuge drum, especially the coating and patterning of photoresist on the interior of a rotating centrifuge drum. The proposed fabrication technique requires deposition of three distinct layers in a centrifuge drum (Figure 1b-d):

(*i*) A planarizing coating of photoresist to improve the drum surface finish

(*ii*) A patterned coating of photoresist to define high resolution features

(*iii*) A polymer layer to produce a stamp casting

First, a layer of photoresist is deposited on the inner surface of a drum by centrifugal coating. The entire layer of photoresist is cured; in the case of a negative photoresist this can be accomplished by uniform exposure. This first step provides a precise and uniform datum surface, regardless of the surface finish of the drum surface.

Downloaded From: http://proceedings.spiedigitallibrary.org/ on 06/17/2015 Terms of Use: http://spiedl.org/terms

Second, another layer of photoresist is deposited on the inner surface of the same drum by centrifugal coating. This photoresist is selectively exposed and developed using a direct write laser system (Figure 2). This patterned layer defines the features that will be transferred to the surface of the final stamp.

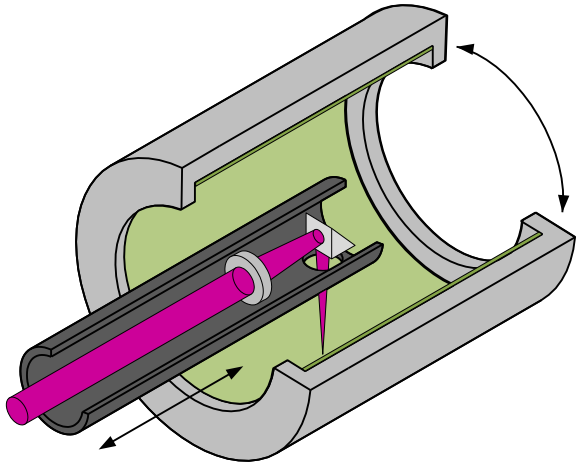

Figure 2: Schematic of UV laser optics for patterning the interior of the centrifuge drum. A single lens element is used to focus the collimated light source on the surface of the drum, redirected through a right angle prism. By rotating the drum and translating the optics along the drum axis, the entire surface of the drum can be exposed.

Third, polymer precursor is deposited on the inner surface of the same drum (for example PDMS precursor). The polymer is allowed to cure while the drum is spinning, which may be accelerated by heating the drum.

The paper is organized to first develop sufficient background surrounding photoresist coating and direct write patterning in the centrifuge drum, then provide experimental details and results from a prototype implementation. Section 2 examines an analytical model of centrifugal photoresist coating to derive appropriate processing parameters. Section 3 describes the design and implementation of the laser direct write system and FPGA controller for direct write patterning in a spinning centrifuge. Section 4 presents the experimental protocol. The results in Section 5 show excellent surface finish from the planarizing layer, good thickness uniformity in the final polymer stamp, and good feature definition from the direct write laser.

2. COATING

In conventional spin coating (e.g. semiconductor processing), photoresist is flooded on a spinning substrate and thinned to a precise layer as the substrate velocity increases. The thickness of the resulting film is dependent on the initial viscosity of the photoresist, spinning speed, spinning time, and solvent volatility.[12] In contrast, the centrifugal coating process used here (Figure 3) relies on conservation of mass to determine the resulting coating thickness. A known volume of diluted photoresist is metered into a slowly spinning drum, which is then ramped to a high speed to produce a uniform fluid surface. After evaporation of the solvent, a uniform thickness of photoresist remains, identically the amount originally dispensed into the drum.

The economy and quality of traditional spin coating depends on spin speed, duration, and photoresist composition. Similarly, the effect of solvent loading must be understood for successful centrifugal coating. Towards this goal, this section derives an analytical model to describe the time required for the dispensed photoresist to reach a perfectly cylindrical fluid surface as shown in Figure 3, Ultimately, this analysis provides guidelines for reasonable fluid properties, film thickness, and centrifuging times to obtain uniform coatings in a centrifuge drum.

Downloaded From: http://proceedings.spiedigitallibrary.org/ on 06/17/2015 Terms of Use: http://spiedl.org/terms

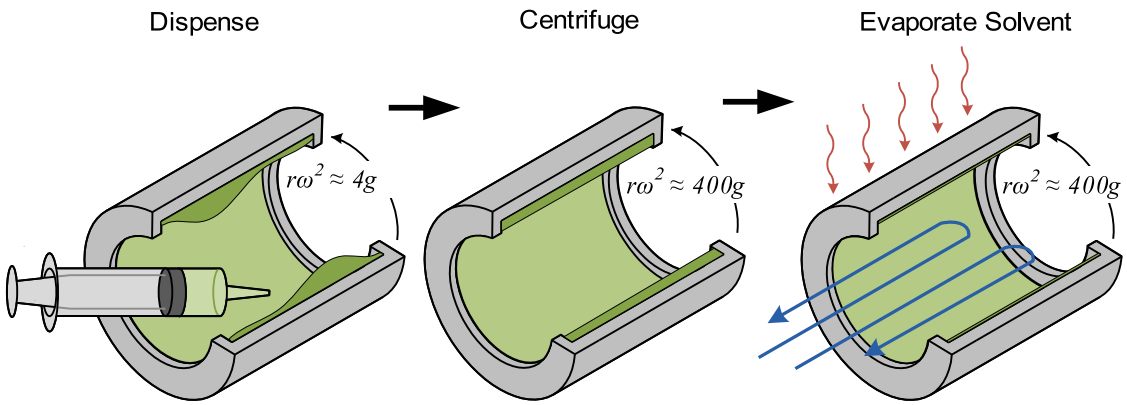

Figure 3: Process map showing centrifugal coating of photoresist. The final resist layer is controlled by metering an exact mass or volume of photoresist and solvent into a slowly spinning centrifuge drum. The drum is ramped up to a high speed to force the mixture to a uniform cylindrical free surface. Finally, the solvent is evaporated through heating and ventilation to leave a uniform thickness of photoresist.

In the ideal case, consider a drum of radius r spinning at a high speed ω creates a large centripetal acceleration $r\omega^2$ that overcomes other forces to provide a uniform free surface (Figure 4a). This centripetal body force on a fluid of density ρ and height h becomes much larger than surface tension σ, resulting in a large Bond number $Bo = \rho r\omega^2 h^2/\sigma$. The large Bond number attenuates surface tension driven edge effects in the steady state fluid surface. Similarly, the centripetal body force becomes much larger than viscous forces in a fluid of kinematic viscosity ν, resulting in a large Galileo number $Ga = r\omega^2 h^3/\nu^2$. The large Galileo number results in faster decay of transient behavior and convergence to the steady state fluid surface. These effects can be leveraged to create exceptionally uniform layers of photoresist and prepolymer on the interior of a centrifuge drum, resulting in a

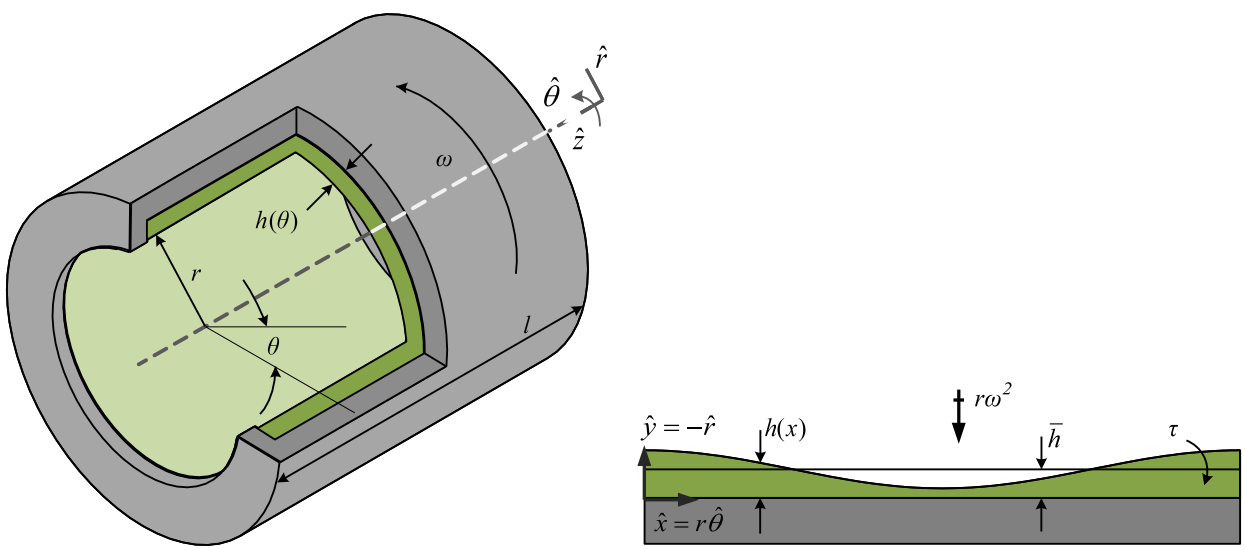

(a) (b)

Figure 4: Notation used in analysis of centrifugal coating and casting. The cylindrical centrifuge drum (a) can be approximated as a fluid layer in Cartesian space (b) for very thin fluid layers. Asperity decay can be analyzed by considering a sinusoidal fluid height profile as shown in (b).

Downloaded From: http://proceedings.spiedigitallibrary.org/ on 06/17/2015 Terms of Use: http://spiedl.org/terms

precise final stamp.

The transient fluid dynamics of the fluid layer are of primary interest, especially the time required for a fluid layer of kinematic viscosity ν and thickness h in a centrifuge drum of radius r operating at speed ω to approach steady state (Figure 4a).

The following analyses assumes that the centripetal acceleration is much greater than gravity ($r\omega^2 \gg g$) and that the fluid layer is everywhere thin ($h \ll r$). Because the fluid layer is very thin, the drum curvature is negligible and the fluid dynamics can be modelled in rectilinear coordinates (coordinate system $\hat{\theta}, \hat{r}$ is converted to $\hat{x}$, $\hat{y}$ as shown in Figure 4b).

Inertial terms are assumed small, permitting application of lubrication theory using the Stokes equations for incompressible flow (the reader is referred to[13] for details). Using the assumption that $h \ll r$ allows eliminating small terms and reducing the Stokes equations to a pair of differential equations in the $\hat{x}$ and $\hat{y}$ directions relating the pressure field p and velocity field $[u, v]$ with dynamic viscosity μ:

$$\hat{x}: \qquad 0 = -\frac{\partial p}{\partial x} + \mu \frac{\partial^2 u}{\partial y^2} \tag{1a}$$

$$\hat{y}: \qquad 0 = -\frac{\partial p}{\partial y} - \rho r \omega^2 \tag{1b}$$

The boundary conditions on the fluid are given by a no-slip condition at the drum interface and zero shear at the free surface:

$$u|_{y=0} = 0 \tag{2}$$

$$\mu \frac{\partial u}{\partial x}\Big|_{y=h(x)} = 0 \tag{3}$$

Additionally, the pressure at the free surface is taken to be zero:

$$p|_{y=h(x)} = 0 \tag{4}$$

Integrating $\partial p/\partial y$ (1b) across the fluid height $h(x)$ with the boundary condition (4) of zero pressure at the free surface gives pressure p as a function of height y:

$$p(x, y) = \rho r \omega^2 (h(x) - y) \tag{5}$$

Differentiating this result gives $\partial p/\partial x$, which enters (1a) as a forcing function. Because $\partial p/\partial x$ is a function of x alone, (1a) can be solved for velocity field u by integration and application of the boundary conditions in (2) and (3):

$$u = \frac{\rho r \omega^2}{\mu} \frac{dh}{dx} \left(\frac{y^2}{2} - y h(x) \right) \tag{6}$$

Next, the volume flow rate Q through a plane in x is given by integrating the flow profile u (6) between 0 and $h(x)$:

$$Q(x) = \int_0^{h(x)} u(x) dy = \frac{\rho r \omega^2}{3\mu} \frac{dh}{dx} h^3(x) \tag{7}$$

Towards achieving a linear differential equation in h, this equation for Q can be simplified if variations in height $h(x)$ are small about $\bar{h}$:

$$Q(x) = \frac{\rho r \omega^2}{3\mu} \frac{dh}{dx} \bar{h}^3(x) \tag{8}$$

Downloaded From: http://proceedings.spiedigitallibrary.org/ on 06/17/2015 Terms of Use: http://spiedl.org/terms

This flow rate Q must be related to the instantaneous change in height profile $h(x)$ to find the rate of decay of sinusoidal asperities (e.g. Figure 4b). Applying a control volume in an infinitesimally small volume about some x coordinate, it can be shown that the temporal derivative of height is related to the spatial derivative of flow rate:[13]

$$\frac{dh}{dt} = -\frac{dQ}{dx} \tag{9}$$

Substituting the volume flow rate Q from (7) gives

$$\frac{dh}{dt} = -\frac{d}{dx}\left(\frac{\rho r \omega^2}{3\mu}\frac{dh}{dx}\bar{h}^3(x)\right) \tag{10}$$

This partial differential equation relates the temporal and spatial aspects of the fluid film profile h. The form of (10) admits a decaying sinusoidal solution for h with wavelength λ:

$$h(x,t) = \bar{h} + e^{-t/\tau}\cos\left(2\pi\frac{x}{\lambda}\right) \tag{11}$$

applying this solution form to (10) and solving for the asperity decay time constant in the fluid layer gives the exponential decay time constant τ as a function of the Galileo number Ga:

$$\tau = \frac{3}{4\pi^2}\frac{\lambda^2}{\nu}Ga^{-1}, \qquad Ga = \frac{r\omega^2\bar{h}^3}{\nu^2} \tag{12}$$

This result shows that sinusoidal height asperities decay as a first order system with a time constant given by (12). One operating rule may be to operate the centrifuge for seven time constants to attenuate asperities by a factor of 1000. For practical coating application, τ must be sufficiently short so that the transient fluid flow decays within a reasonable amount of time.

PDMS, a typical stamp material, has kinematic viscosity $\nu = 3360$ cSt (Dow Corning Sylgard 184). Assuming an asperity wavelength of $\lambda = 2\pi r$, this fluid will have a decay time constant $\tau = 3$ s for a 1 mm fluid layer in a 50 mm diameter centrifuge operating at 300 rad/s.

Photoresist presents a larger challenge. The desired photoresist thickness for patterning features is typically on the order of microns, which results in a very small Galileo number Ga. For example, at typical photoresist is SU8 2015 with a viscosity $\nu = 1250$ cSt. In the same centrifuge drum (50 mm diameter operating at 300 rad/s), a 10 μm layer of SU8 2015 has a decay time constant τ of 12 days. To overcome this prohibitively long transient period, photoresist can be diluted with solvent well beyond the concentrations typically used for spin coating. The solvent both (*i*) lowers the fluid viscosity ν and (*ii*) increases the mean layer thickness $\bar{h}$, both of which act to increase Ga and decrease τ. Once the fluid layer has found equilibrium, the solvent is evaporated to leaving a uniform layer of photoresist. As an example, diluting the same SU8 2015 layer 10:1 with cyclopentanone ($\nu = 1.35$ cSt) gives a decay time constant τ of less than one second.

3. EXPOSURE

Photoresist patterning requires selective exposure to an ultraviolet (UV) light source. Depending on the resist, this exposure will cause cause either cross linking or degradation so that the pattern can be developed in a solvent.

A direct write laser system is designed for this machine. A set of focusing optics are used to direct a collimated laser beam to a small spot on the inner surface of the centrifuge drum. The ultimate patterning resolution of the system will be dictated by the minimum spot diameter achievable.

A laser direct write scheme is used in this system to provide the flexibility of producing arbitrary stamp patterns in photoresist. This application presents challenges not encountered in traditional direct write systems

Downloaded From: http://proceedings.spiedigitallibrary.org/ on 06/17/2015 Terms of Use: http://spiedl.org/terms

for planar substrates, especially space constraints. The architecture shown in Figure 2 was selected to allow patterning of arbitrarily sized centrifuge drums: a light source is supplied coaxially with the centrifuge drum, then diverted to the surface of the drum where desired. At the same time, a set of focusing optics are used to direct a collimated laser beam to a small spot on the drum surface; the ultimate patterning resolution of the system will be dictated by the focused spot diameter.

3.1 Gaussian Beam

Laser beams are characterized by a Guassian profile: the irradiance (power density) follows a bell shaped distribution with the maximum intensity at the center of the beam. The irradiance profile I is given as a function of radius r from the beam axis:[14]

$$I(r) = I_0 e^{-2r^2/w^2} \tag{13}$$

where I_0 is the irradiance at the beam axis and w is the characteristic radius of the beam (Figure 5a). From this relationship, it is clear that w is the radius at which $I(r)$ drops to $1/e^2$ (or 14%) of the maximum I_0.

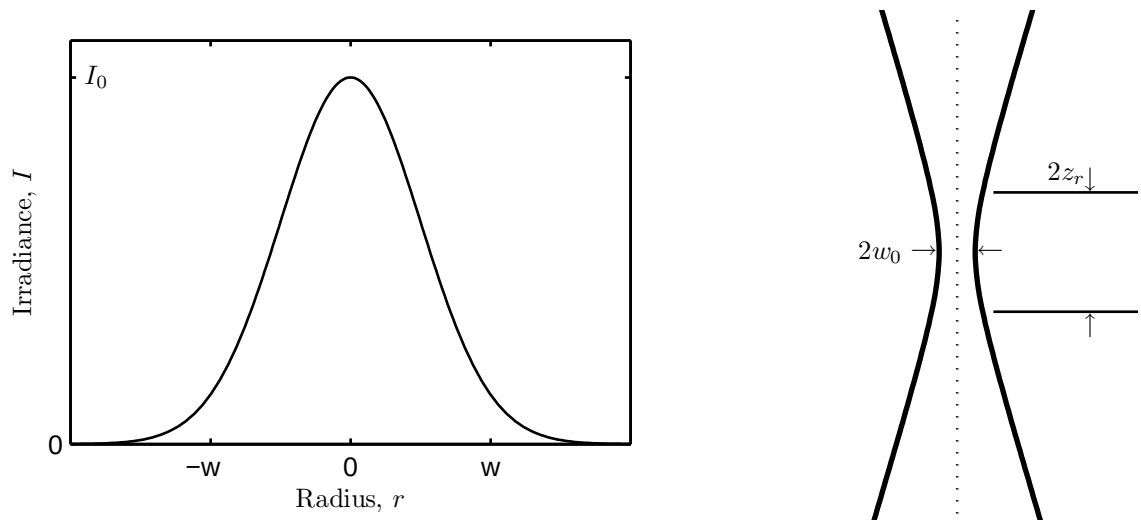

(a) (b)

Figure 5: (a) Gaussian beam irradiance profile; the beam irradiance drops from its maximum power density I_0 to I_0/e^2 at the characteristic beam radius w. (b) A beam with a convergence angle of Θ with have a Rayleigh range z_r and a waist radius w_0.

Focusing a Gaussian beam results in a finite spot size determined by diffraction limits (Figure 5b). The profile $w(z)$ of the beam radius along the beam axis $\hat{z}$ is given by[14]

$$w(z) = w_0 \left[1 + \left(\frac{\lambda z}{\pi w_0^2} \right)^2 \right]^{1/2} \tag{14}$$

where the minimum radius w_0 at the beam waist is a function of wavelength λ and beam divergence angle Θ:

$$w_0 = 1.22 \frac{\lambda}{\Theta} \tag{15}$$

Integrating the irradiance profile over the beam area gives the total transmitted power P:

$$P = \frac{1}{2} \pi I_0 w^2 \tag{16}$$

Downloaded From: http://proceedings.spiedigitallibrary.org/ on 06/17/2015 Terms of Use: http://spiedl.org/terms

Table 1: Direct write laser specifications

Specification	Value
Power, P	80 mW
Wavelength, λ	405 nm
Beam diameter, D	6 mm
Maximum trigger frequency	1 MHz

The *Rayleigh range* is where the beam area doubles, or equivalently the radius increases by $\sqrt{2}$:

$$z_R = \frac{\pi w_0^2}{\lambda} \tag{17}$$

The depth of focus (centered about the beam waist) is typically considered $2z_r$ (twice the Rayleigh range).

The relationship in (17) shows the primary tradeoff in laser focusing: smaller spot diameters result in a smaller depth of focus. In other words, a higher resolution system becomes increasingly sensitive to the relative positioning of the optics and desired image plane. In the case of this direct write system, a smaller depth of focus requires higher accuracy in the positioning of the optics and centrifuge drum.

3.2 Optical Design

A single element focusing system is designed for direct write operations in the centrifuge drum (Figure 6a). In this relatively simple architecture, a single plano-convex lens is used to focus a collimated laser beam to a single spot.

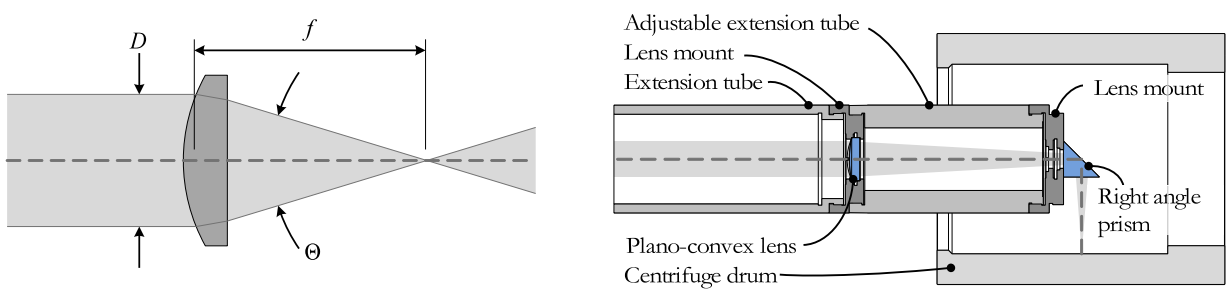

(a) (b)

Figure 6: (a) Single element focusing architecture using a single plano-convex lens to focus a collimated laser beam to a concentrated spot. Characteristic dimensions used in the design analysis are shown. (b) Single optical element implementation using C-mount components. The beam travels through a stack of C-mount components located coaxially with the centrifuge drum. A right angle prism is used to redirect the focused beam towards the drum surface. In designs with shorter focal lengths, the focusing element can be located on the opposite side of the prism.

The Guassian beam waist equations can be rewritten in terms of design variables, where D is the collimated laser beam diameter and f is the focal length of the lens. A 405 nm wavelength, 80 mW power laser with a 6 mm beam diameter was selected as a light source (Table 1).

For this prototype design, a lens with focal length $f = 75$ mm was chosen to provide reasonably small spot size ($2\omega_0 = 12$ μm) while still providing a relatively large depth of focus ($2z_r = 0.6$ mm). This large depth of focus allows robust operation without closed loop focus control despite a drum runout of about 15 μm and an uncertainty in resist thickness of about 10 μm.

Standard C-mount components were used to build the optics assembly. An adjustable body tube was placed between the lens element and the prism to adjust the beam focus to the drum surface.

Downloaded From: http://proceedings.spiedigitallibrary.org/ on 06/17/2015 Terms of Use: http://spiedl.org/terms

3.3 Machine Integration

The centrifuge drum and laser optics must be capable of relative motion to pattern the entire drum surface. Cylindrical motion coordinates are used as shown in Figure 2, where the drum is able to spin in its own bearings (along $\hat{\psi}$) and the laser optics travel on a motion stage along the drum axis ($\hat{z}$). These two degrees of freedom allow patterning the entire area of the centrifuge drum at a constant radius r.

The centrifuge and focusing optics must be precisely aligned, but should also be fixed in such a way to allow disassembly. Each component must be removable, for example to allow draining solvent from the centrifuge drum. To this end, the centrifuge and laser optics are located to the machine base using three groove kinematic couplings (Figure 7a).

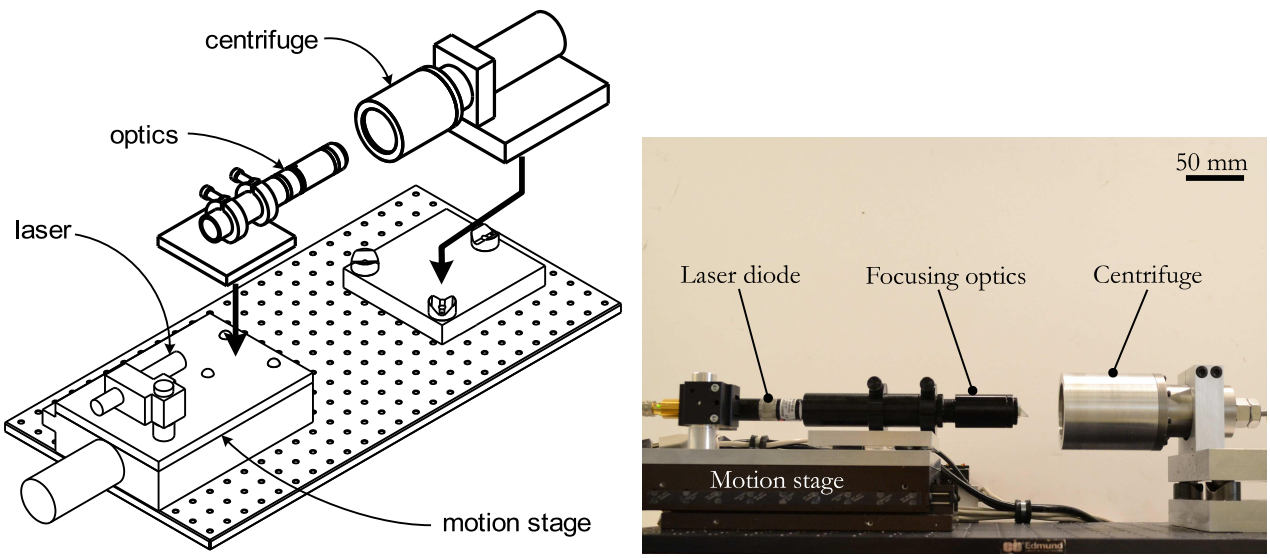

(a) (b)

Figure 7: (a) Schematic of direct write system, showing removal of laser optics and centrifuge drum from their kinematic mounts. (b) Photograph of machine for producing cylindrical stamps. A UV laser and focusing optics are mounted on a linear motion stage for motion along the axis of a horizontal centrifuge drum.

The assembled machine is shown in Figure 7b, where the position of the laser optics along the axis of the centrifuge drum can clearly be seen.

3.4 Control

The centrifuge and laser positioning stage were driven with DC servo motors with quadrature encoders. The encoders, power amplifiers, and laser were interfaced with a National Instruments PCIe-7852R FPGA data acquisition card. The FPGA was used for closed loop control of the servo axes and for precise timing of the laser using a 10 MHz clock.

The centrifuge was operated at constant velocity, while the laser motion stage was position controlled. Exposure was performed at discrete z steps by stepping the motion stage in small increments. The FPGA was programmed to pulse the laser in sequence with the centrifuge quadrature encoder to expose a pattern of dashed lines around the centrifuge.

With a more sophisticated controller design, the same hardware would be capable of a spiral write trajectory (faster than a cylindrical step and repeat trajectory) and arbitrary pattern generation from bitmap images.

Downloaded From: http://proceedings.spiedigitallibrary.org/ on 06/17/2015 Terms of Use: http://spiedl.org/terms

4. EXPERIMENTAL METHOD

The stamp production process was performed in a centrifuge drum with an internal cavity 60 mm long and 52.8 mm in diameter. This drum produced a 1 mm thick stamp that can be fit to a 50.8 mm diameter printing roller.

Each of the layers shown in Figure 1 were applied using the described centrifugal coating process shown in Figure 3. Fluids were introduced at a drum speed of 50 rad/s to avoid turbulence, after which the drum was accelerated to 300 rad/s at 50 rad/s/s. Heating was achieved using a heat gun directed at the centrifuge drum; a thermocouple was used to monitor the air temperature near the spinning drum.

SU8 photoresist was used as the planarizing layer (Figure 1b) because of its excellent adhesion to aluminum and high chemical and temperature resistance. A volume of 0.5 mL SU8 2015 (Microchem) was diluted in a beaker with 5 mL cyclopentanone (Microchem) and mixed with a stirring rod. The mixture was centrifuged for 60 s, then heated to 95 C until all solvent had evaporated. The remaining SU8 layer was uniformly exposed with 405 nm UV light emitting diodes at an exposure dose of 7500 mJ/cm^2. The exposed film was baked at 95 C for 15 minutes to crosslink the SU8, then at 150 C for 15 minutes for improved adhesion to the aluminum drum.

SPR 220 photoresist was used as the patterning layer (Figure 1c) because it remains highly responsive at the 405 nm laser wavelength. A volume of 0.1 mL SPR 220-3.0 (Dow Corning) was diluted in a beaker with 5 mL of 2:1 ethyl lactate (Sigma Aldrich) and anisol (Sigma Aldrich) and mixed with a stirring rod. The mixture was centrifuged for 60 s, then heated to 115 C while aerating with compressed air until all solvent had evaporated. After cooling to 25 C, the remaining layer of SPR 220 was selectively exposed with the laser. Exposure at each axial coordinate was performed in a single rotation of the centrifuge drum at an energy level of 200 mJ/cm^2, requiring only 50 ms. The exposed film was baked at 115 C for 2 minutes and cooled. The pattern was developed under a stream of MF-24A (Dow Corning) for one minute and rinsed with dionized water.

PDMS was used as the stamp polymer (Figure 1d). Sylgard 184 (Dow Corning) was mixed at a 10:1 ratio and degassed under vacuum for 10 minutes. A syringe was used to meter 10 mL of PDMS into the centrifuge. The PDMS was centrifuged for 5 minutes, then heated to 65 C for 60 minutes to cure.

Several PDMS stamps could be cast against the planarizing and patterning layers without observable degradation. It was found that a single planarizing layer could be reused many times for different stamp designs by removing the SPR 220 patterning layer with an organic solvent (e.g. acetone) that left the SU8 intact, then recoating and developing a new layer of SPR 220.

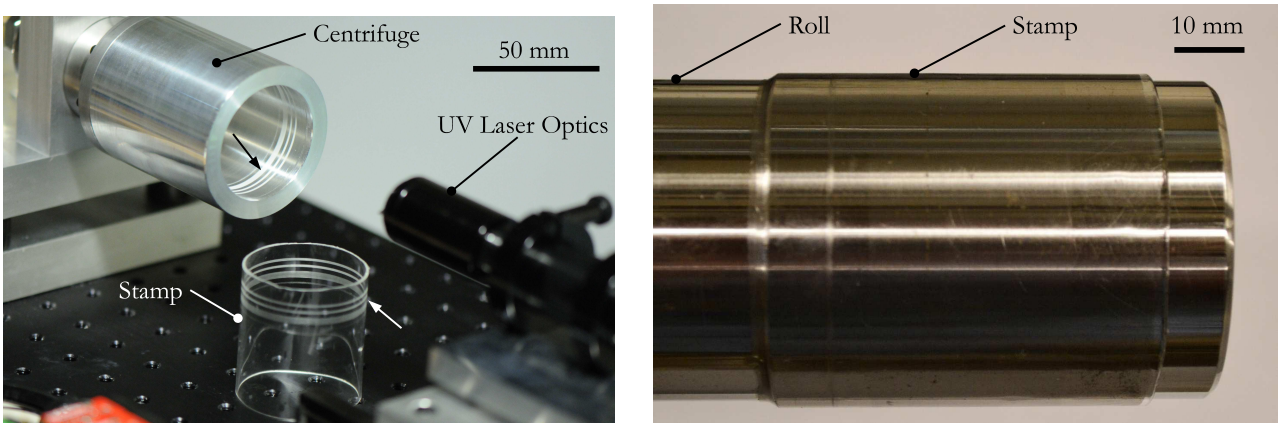

(a) (b)

Figure 8: (a) A 50 mm diameter cylindrical stamp shown with prototype machine, including centrifuge drum and a UV laser for patterning. Grating patterns on the inner diameter of the drum are replicated in the outer diameter of the stamp (arrows). (b) A similar stamp mounted to a roll for use as a roll-to-roll printing tool. A lubricating layer of pressurized air or solvent is used to slide the stamp over the roll.

After curing, the stamp was removed from the drum (Figure 8a) and either used for measurements or mounted to a roll for printing (Figure 8b).

Downloaded From: http://proceedings.spiedigitallibrary.org/ on 06/17/2015 Terms of Use: http://spiedl.org/terms

5. RESULTS

5.1 Surface Roughness

The surface roughness of each photoresist layer was determined by characterizing the corresponding PDMS stamp surface. Measurements of multiple samples with a white light interferometer indicate that the SU8 coatings achieve about 20 nm RMS surface roughness, while the SPR 220 coatings achieve about 10 nm RMS surface roughness. The SU8 planarizing layer gave no evidence of the underlying machining marks in the aluminum centrifuge drum (Figure 9).

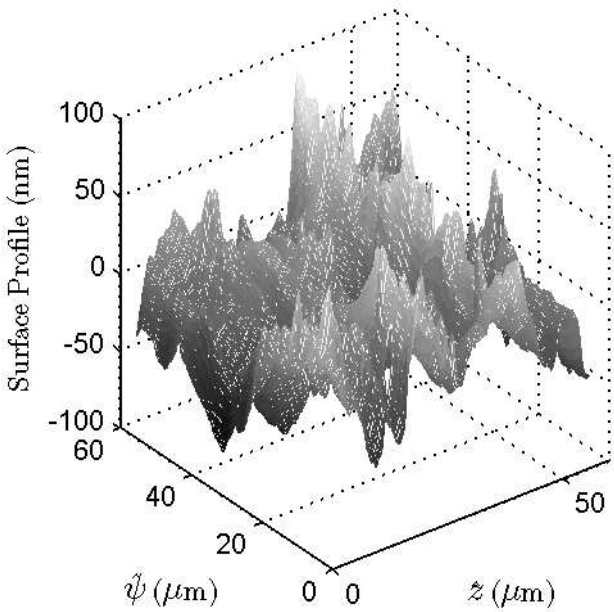

Figure 9: Surface map of planarizing layer showing 22 nm RMS roughness, as measured from a replicated PDMS stamp surface.

5.2 Patterning

The ability to produce individual stamp features was demonstrated by triggering the laser output with the centrifuge encoder (4000 pulses per revolution; one pulse every 40 μm of drum perimeter). Using this technique, lines with a 40 μm half pitch were written every 50 μm along the drum axis. The resulting 40 $\times$ 10 μm features are shown in figures 10a-10b.

Downloaded From: http://proceedings.spiedigitallibrary.org/ on 06/17/2015 Terms of Use: http://spiedl.org/terms

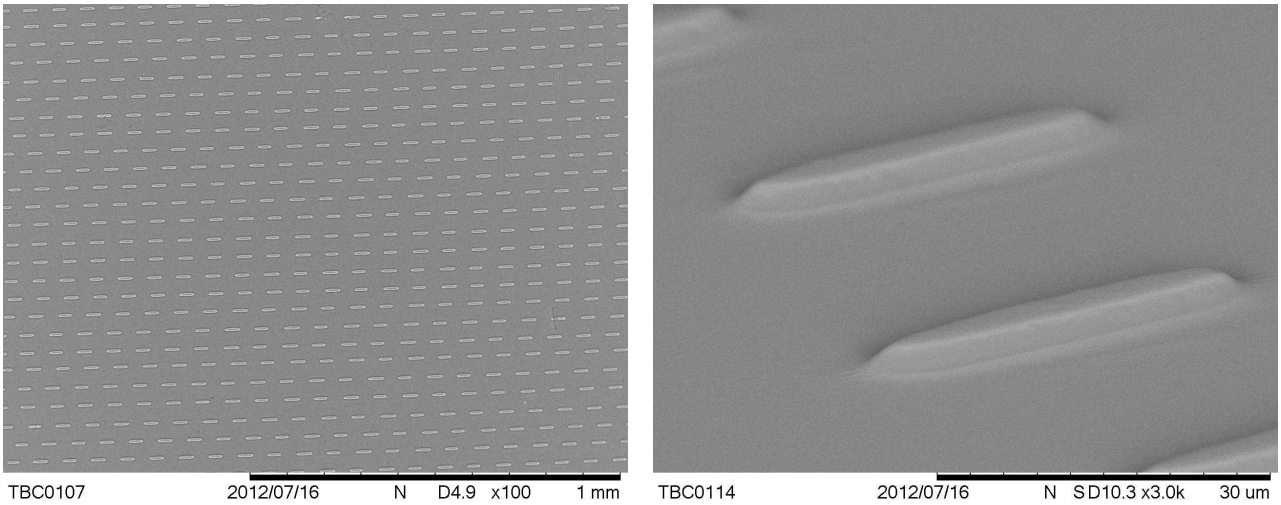

(a) (b)

Figure 10: (a) SEM micrograph showing a field of individual stamp features created by writing laser pulses in the patterned photoresist layer. The vertical direction in this micrograph is along the $\hat{z}$ axis of the stamp. (b) Detail of individual features in a PDMS stamp replicated from photoresist patterned inside the centrifuge drum.

5.3 Thickness

The thickness uniformity of the resulting PDMS stamps was measured by sampling 2 mm diameter cores at multiple locations (Figure 11a). These samples were mounted to a glass microscopy slide by floating on a layer of ethanol. After the ethanol evaporated, the samples were left in contact with the microscopy slide in a stress-free condition (Figure 11b).

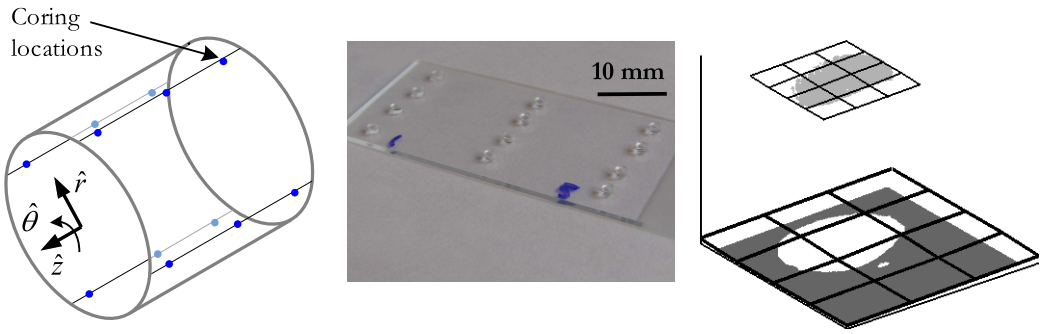

(a) (b) (c)

Figure 11: Stamp thickness was measured using cores samples. (a) Cores were sampled from three different axial locations at orthogonal angular coordinates. (b) Cores were mounted to a microscopy slide for interferometry measurements. (c) Stamp thickness is determined as the height difference between the slide and core top in interferometry data (best fit planes shown for clarity).

The height difference between the glass slide and top surface of the stamp core was measured using a white light interferometer. A plane was fit to the data points corresponding to the glass slide. The height of the core was measured as the mean distance between this plane and the remaining data points. The thickness residual at each coring point was calculated as the difference between each measurement and the mean of all measurements in the stamp. An analysis of variance (ANOVA) across three sets of measurements showed the standard deviation

Downloaded From: http://proceedings.spiedigitallibrary.org/ on 06/17/2015 Terms of Use: http://spiedl.org/terms

of measurement to be 1.93 μm.

Figure 12 shows the thickness residual distribution of a typical 1 mm thick stamp. These data indicate both a taper and an eccentricity in the stamp. The mean residual steadily decreases as a function of axial position, indicating a taper of about 340 μrad (17 μm over 50 mm). Eccentricity of 2 μm is indicated by the geometric mean of each axial data set, plotted in the center of Figure 12.

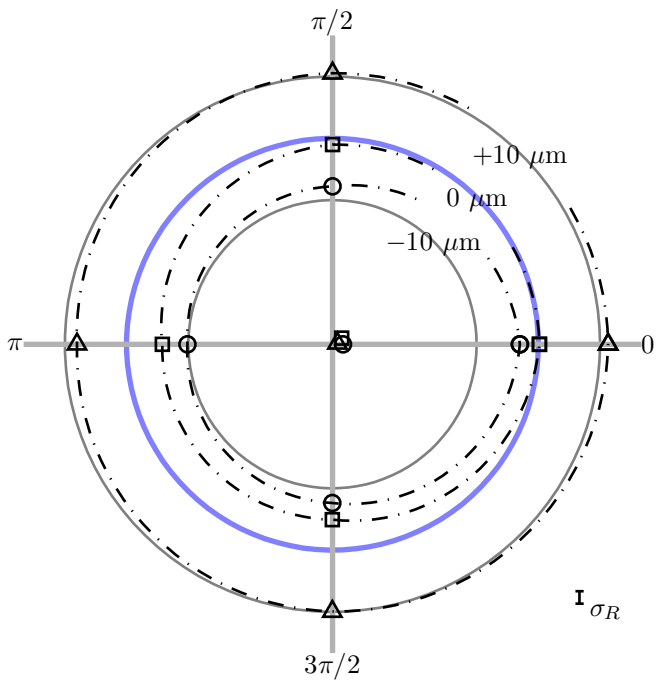

Figure 12: Typical stamp thickness residual for a 1 mm thick stamp, shown as a function of axial position $\hat{z}$ for positions (◯) 5 mm, (□) 30 mm, and (△) 55 mm from the open face of the centrifuge drum. The geometric mean of each data set is plotted near the origin, indicating eccentricity. The data suggests a taper of 17 μm and an eccentricity of 2 μm; the measurement repeatability $\sigma_R = 2\ \mu$m is shown on the chart for comparison.

6. DISCUSSION AND CONCLUSION

This initial demonstration of polymer stamps fabricated by centrifugal casting shows good feature resolution and stamp uniformity. Line widths of 10 μm were written in photoresist with a direct write technique and replicated in a PDMS stamp. Stamp thickness measurements show that the final stamp has very little eccentricity and a taper of 340 μrad.

The planarizing layer effectively reduced the surface roughness of the drum to about 10 nm RMS. The stamp thickness data suggests that the planarizing layer also removes larger geometric errors in the drum; for example the original 15 μm drum runout was reduced to a 2 μm measured eccentricity in the final stamp.

The patterning layer demonstrates the efficacy of a direct write technique inside a centrifuge drum. The 10 μm line widths demonstrated in this paper were provided by a conservative design of laser focusing optics; it is expected that the ultimate resolution of this technique will be at the optical diffraction limit. An improved machine will provide a higher degree of patterning accuracy than observed in these results shown in figures 10a-10b.

It is hypothesized that the taper in the stamp thickness is primarily caused by a taper in the drum that the planarizing layer was unable to completely attenuate. It is expected that 1 μm tolerances can be achieved on the stamp thickness uniformity through more precise machinery and improved understanding of the coupled fluid

Downloaded From: http://proceedings.spiedigitallibrary.org/ on 06/17/2015 Terms of Use: http://spiedl.org/terms

dynamics and mass transfer during photoresist solvent evaporation (a common phenomenon observed in spin coating of photoresists).

These experiments were conducted using PDMS as the stamp material. It is anticipated that this method can be adapted to produce stamps in harder polymers (e.g. polyurethanes or fluoropolymers) with little difficulty. While PDMS functions well for microcontact printing and flexography, these harder polymers are more amenable for imprinting processes.

From these results, we conclude that this centrifugal stamp casting technique is a promising approach towards precision cylindrical stamps for roll-based lithography. The fluid dynamics of the coating process have no inherent scaling limitations; it is expected that this process would successfully scale to roll widths of one meter. This process can be quite economical; a single master drum can be patterned with planarizing and patterning layers of photoresist and subsequently used to produce many identical polymer stamps. Moreover, the planarizing layer permits use of as-machined centrifuge drums without expensive surface finishing operations. While the use of a UV light source precludes features at the single nanometer scale, the resulting microfeatured stamps will be appropriate for applications in flexible electronics, flexible displays, and engineering metasurfaces.

ACKNOWLEDGEMENTS

The authors gratefully acknowledge support from and collaboration with the King Faud University of Petroleum and Minerals within the Center for Clean Water and Energy at MIT and KFUPM. The authors also thank National Instruments for donation of data acquisition hardware.

REFERENCES

[1] Ahn, S. and Guo, L., "Large-area roll-to-roll and roll-to-plate nanoimprint lithography: a step toward high-throughput application of continuous nanoimprinting," *ACS Nano* **3**(8), 2304–2310 (2009).

[2] Xia, Y. and Whitesides, G. M., "Soft Lithography," *Angewandte Chemie International Edition* **37**, 550–575 (Aug. 1998).

[3] Dumond, J. J. and Low, H. Y., "Recent developments and design challenges in continuous roller micro- and nanoimprinting," *Journal of Vacuum Science and Technology B: Microelectronics and Nanometer Structures* **30**(1), 010801 (2012).

[4] Chen, L., Yen, J., Chen, Y., Wang, L., Chung, T., Lin, H., Chen, P., and Chang, S., "Longitudinal stitching of sub-micron periodic fringes on a roller," *Microelectronic Engineering* **88**(11), 3235–3243 (2011).

[5] Kim, S. and Kim, G., "Micropatterning on roll surface using photo-lithography processes," *International Journal of Precision Engineering and Manufacturing* **12**, 763–768 (2011).

[6] Idei, K., Ishizawa, N., Noda, D., and Hattori, T., "Development of roll metal mold by synchrotron radiation," in [*Micro-NanoMechatronics and Human Science, 2006 International Symposium on*], 1 –6 (nov. 2006).

[7] Taniguchi, J. and Aratani, M., "Fabrication of a seamless roll mold by direct writing with an electron beam on a rotating cylindrical substrate," **27**(6), 2841–2845, AVS (2009).

[8] Unno, N. and Taniguchi, J., "Fabrication of the metal nano pattern on plastic substrate using roll nanoimprint," *Microelectronic Engineering* **88**(8), 2149 – 2153 (2011).

[9] Unno, N., T. J. I. K., "Fabrication of a seamless roll mold using inorganic electron beam resist with postexposure bake," *Journal of Vacuum Science and Technology B: Microelectronics and Nanometer Structures* **29**(6) (2011).

[10] Petrzelka, J. E. and Hardt, D. E., "Limitations on roll based microcontact printing imposed by variations in macro scale stamp dimensions," in [*2011 MRS Fall Meeting*], (2011).

[11] Petrzelka, J. and Hardt, D., "Roll based soft lithography: Stamp contact mechanics and process sensitivity," *ASME Journal of Manufacturing Science and Engineering* , submitted.

[12] Flack, W. W., Soong, D. S., Bell, A. T., and Hess, D. W., "A mathematical model for spin coating of polymer resists," *Journal of Applied Physics* **56**(4), 1199–1206 (1984).

[13] Petrzelka, J. E., phd thesis, Massachusetts Institute of Technology (2012).

[14] Hecht, E., [*Optics*], Addison-Wesley, Reading, Mass., 3rd ed. ed. (1998).

Downloaded From: http://proceedings.spiedigitallibrary.org/ on 06/17/2015 Terms of Use: http://spiedl.org/terms